Supplementary Information

Comparison of Contribution to Phase Boundary from A-site Aliovalent Dopant in High-performance KNN-based Ceramics

Lin Zhao[1], Wenjuan Wu[2], Chunlin Zhao[3], Bo Wu[1], Jian Ma[1] and Hong Tao*[1]

[1]Sichuan Prov Key Lab Informat Mat, Southwest Minzu University, Chengdu 610041, China.

[2]Sichuan Province Key Laboratory of Information Materials and Devices Application, Chengdu University of Information Technology, Chengdu, Sichuan, China

[3]Department of Materials Science, Fuzhou University, Fuzhou, 310002, China

*** Corresponding author:** taohongscu@163.com

1. Structure analysis

Figure S1 shows the grain size distribution of the ceramics with *x*=0.010, 0.015 and 0.020. Figure S2 shows the Rietveld refinement of XRD patterns when 2*θ*=10-90°. It can be seen that well-matched refined results are gained for the ceramics when *x* changes from 0.010 to 0.020. And the low sig and R_w values are presented in Table S1 along with structure parameters.

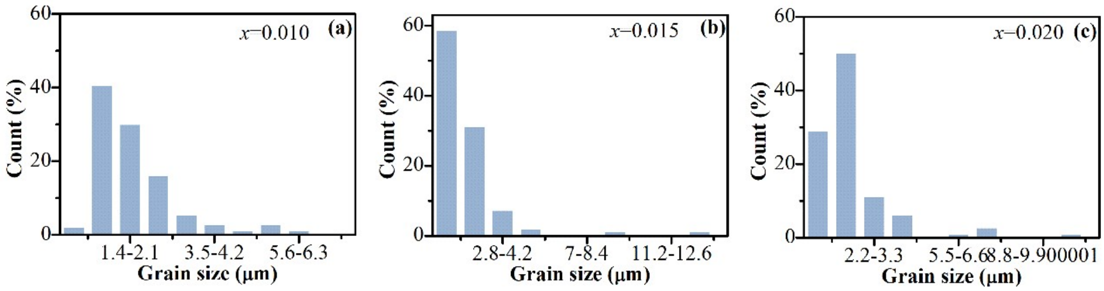

Figure S1. Grain size distribution of the ceramics: (a) *x*=0.010, (b) *x*=0.015, (c) *x*=0.020.

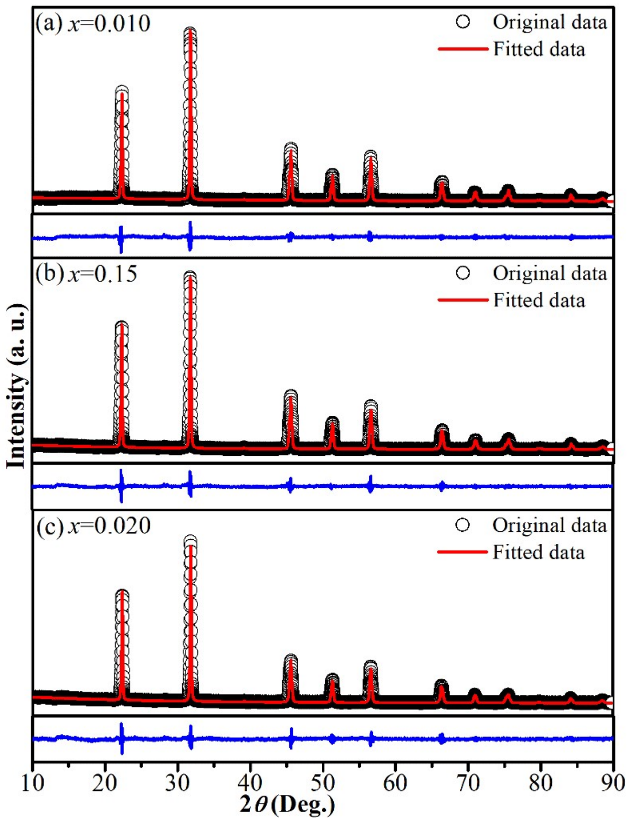

Figure S2. Rietveld refinement of XRD patterns for the ceramics when 2*θ*=10-90°: (a) *x*=0.010, (b) *x*=0.015, (c) *x*=0.020.

Table S1. Structure parameters for the ceramics with different compositions, measured at 25 °C.

x	sig	R_w (%)	Space group	a (Å)	b (Å)	c (Å)	Alpha(°)
			R3m	3.9873	3.9873	3.9873	89.9034
0.010	1.94	2.42	Amm2	3.9732	5.6439	5.6601	-
			P4mm	3.9750	3.9750	3.9979	-
			R3m	3.9907	3.9907	3.9907	89.6313
0.015	1.71	2.09	Amm2	3.9701	5.6450	5.6886	-
			P4mm	3.9722	3.9722	3.9942	-
			R3m	3.9860	3.9860	3.9860	89.7461
0.020	1.60	2.06	Amm2	3.9715	5.6946	5.6318	-
			P4mm	3.9714	3.9714	3.9914	-

2. Electrical properties

Figure S3 shows the *P-E* and *I-E* loops of the ceramics with different compositions. The saturated loops maintained with little changed P_{max} and P_r with increasing Ca^{2+} and reducing Bi^{3+}, while a slight decline happens for E_C. And the electric current peaks induced by domain switching shift to lower electric field, corresponding to the lowered E_C.

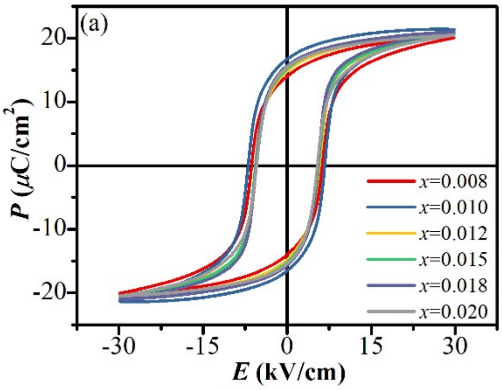

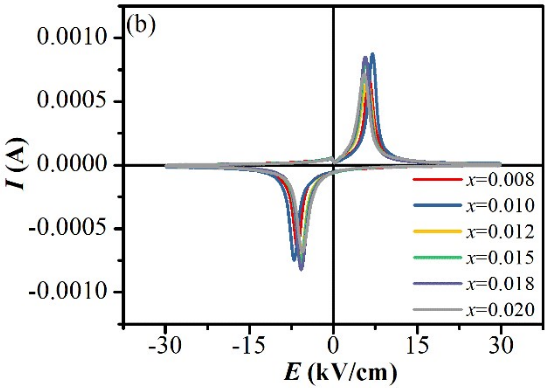

Figure S3. (a) *P-E* loops and (b) *I-E* curves of the ceramics

3. Temperature stability

Figure S4 shows *P-E* loops for the ceramics measured at different temperatures. One can see the *P-E* loops gradually become slim with increasing temperature, implying reduced P_{max} and P_r values which originate from lowered polarization and difficult orientation of dipoles under thermal disturbance. And the E_C decreases because of the increased activity under thermal field.

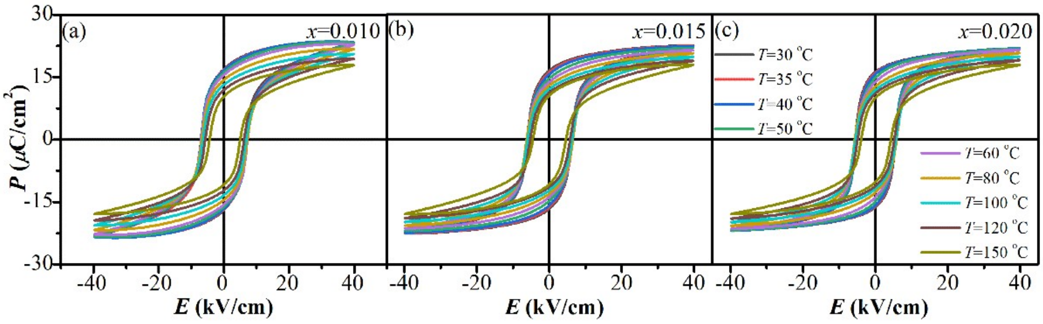

Figure S4. Temperature-dependent *P-E* loops: (a) *x*=0.010, (b) *x*=0.015, (c) *x*=0.020. 、

Figure S5 shows the small signal d_{33} curves of the ceramics measured at different temperatures. The vertical coordinates at zero electric field is the small signal d_{33} values after poling. Obviously, the small signal d_{33} depends on temperature, which is due to the closely relationship between temperature and polycrystalline phase boundary in KNN-based ceramics.

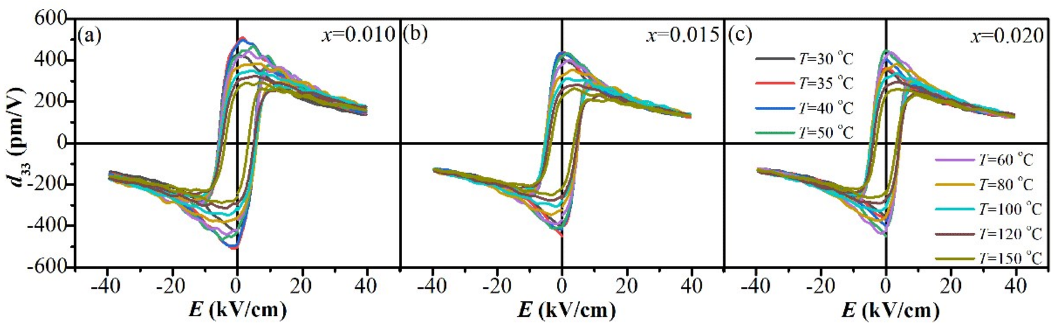

Figure S5. Temperature-dependent small signal d_{33} curves: (a) x=0.010, (b) x=0.015, (c) x=0.020.

Figure S6 shows the bipolar and unipolar strain curves of the ceramics measured at different temperatures. According to bipolar strain curves [Fig. S6(a)~(c)], both s_{pos} and s_{neg} is related to temperature. And s_{uni} show similar values and change tendency to s_{pos}, as seen in Fig. S6(d)~(f). The temperature dependence of strain is owing to the temperature-related converse piezoelectric effect, non-180^o domain switching, domain wall motion, electrostriction, and possible electric field-induced phase transition [1, 2].

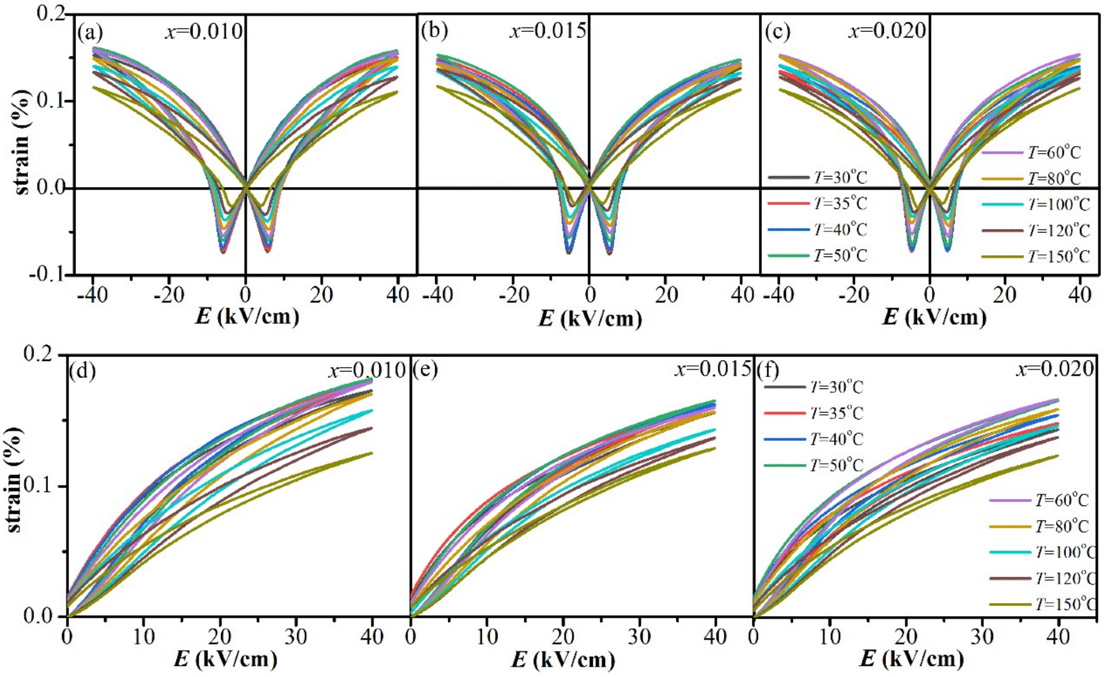

Figure S6. Temperature-dependent bipolar strain curves: (a) x=0.010, (b) x=0.015, (c) x=0.020; temperature-dependent unipolar strain curves: (d) x=0.010, (e) x=0.015, (f) x=0.020.

Reference

[1] X. Lv, J. G. Zhu, D. Q. Xiao, X. X. Zhang, J. G. Wu, Emerging new phase boundary in potassium sodium-niobate based ceramics, *Chem. Soc. Rev.,* 2020, 49, 671-707.

[2] C. L. Zhao, B. Wu, K. Wang, J. F. Li, D. Q. Xiao, J. G. Zhu, J. G. Wu, Practical high strain with superior temperature stability in lead-free piezoceramics through domain engineering. *J. Mater. Chem. A.,* 2018, 6, 23736–23745.